

*Geology*  
*Geology fields*

---

Okayama University

Year 2004

---

A theoretical interpretation of the  
chemical shift of Si-29 NMR peaks in  
alkali borosilicate glasses

Tokuro Nanba\*      Mitsunori Nishimura<sup>†</sup>  
Yoshinari Miura<sup>‡</sup>

\*Okayama University, tokuro.n@cc.okayama-u.ac.jp

<sup>†</sup>Okayama University

<sup>‡</sup>Okayama University

This paper is posted at eScholarship@OUDIR : Okayama University Digital Information Repository.

[http://escholarship.lib.okayama-u.ac.jp/geology\\_general/1](http://escholarship.lib.okayama-u.ac.jp/geology_general/1)

## A theoretical interpretation of the chemical shift of $^{29}\text{Si}$ NMR peaks in alkali borosilicate glasses

Tokuro Nanba,\* Mitsunori Nishimura, and Yoshinari Miura  
Okayama University, Okayama, Japan 700-8530

\* Author to whom correspondence should be addressed([tokuro\\_n@cc.okayama-u.ac.jp](mailto:tokuro_n@cc.okayama-u.ac.jp)).

Abstract—In  $^{29}\text{Si}$ -NMR, it has so far been accepted that the chemical shifts of  $Q^n$  species ( $\text{SiO}_4$  units containing  $n$  bridging oxygens) were equivalent between alkali borosilicate and boron-free alkali silicate glasses. In the sodium borosilicate glasses with low sodium content, however, a contradiction was confirmed in the estimation of alkali distribution;  $^{11}\text{B}$  NMR suggested that Na ions were entirely distributed to borate groups to form  $\text{BO}_4$  units, whereas a  $-90$  ppm component was also observed in  $^{29}\text{Si}$ -NMR spectra, which has been attributed to  $Q^3$  species associated with a non-bridging oxygen (NBO). Then, cluster molecular orbital calculations were performed to interpret the  $-90$  ppm component in the borosilicate glasses. It was found that a silicon atom which had two tetrahedral borons (B4) as its second nearest neighbors was similar in atomic charge and Si2p energy to the  $Q^3$  species in boron-free alkali silicates. Unequal distribution of electrons in Si–O–B4 bridging bonds was also found, where much electrons were localized on the Si–O bonds. It was finally concluded that the Si–O–B4 bridges with narrow bond angle were responsible for the  $-90$  ppm  $^{29}\text{Si}$  component in the borosilicate glasses. There still remained another interpretation; the  $Q^3$  species were actually present in the glasses, and NBOs in the  $Q^3$  species were derived from the tricluster groups, such as  $(\text{O}_3\text{Si})\text{O}(\text{BO}_3)_2$ . In the glasses with low sodium content, however, it was concluded that the tricluster groups were not so abundant to contribute to the  $-90$  ppm component.

## 1. INTRODUCTION

In oxide glasses such as silicate glass, oxide ions are generally classified into bridging oxygen (BO) and nonbridging oxygen (NBO). When an alkali oxide,  $R_2O$  is added to silica,  $SiO_2$ ,  $Si-O-Si$  bridging networks were dissociated to form NBOs, where each alkali ion is adjoined by an NBO for valence compensation. It is widely known that the addition of  $Al_2O_3$  or  $B_2O_3$  is effective in improving chemical durability and mechanical strength of the glass. With increasing  $Al_2O_3$  content, NBO decreases along with the alternative formation of tetrahedral  $AlO_4$  units, and NBO disappears at  $R_2O/Al_2O_3$  ratio = 1, where alkali ions compensate the negative charge of  $AlO_4$  units (Scholze, 1991). In case of the  $B_2O_3$  addition, however, the situation is quite different; Yun and Bray (1978) revealed from  $^{11}B$  nuclear magnetic resonance (NMR) studies of  $RNa_2O \cdot B_2O_3 \cdot KSiO_2$  glasses that NBO is present even at  $R = 1$ . It is due to the difference in preferential coordination structure between B and Al; in glassy state part of borons always occupy the trigonal  $BO_3$  site, and the fraction of fourfold coordinated borons ( $N_4$ ) is less than 1.

From the viewpoint of valence compensation, alkali ions are distributed to the following negatively-charged structural species;  $BO_4$  units and NBOs in  $SiO_4$  and  $BO_3$  units. Various alkali distribution models have been proposed by Dell et al. (1983) and Zhong et al. (1988) from  $^{11}B$  NMR, MacKenzie et al. (1994) from  $^{29}Si$  magic angle spinning (MAS) NMR, and Miura et al. (2001) from X-ray photoelectron spectroscopy (XPS). However, these models have been applied only to their own experimental results and have not been tested using the experimental data collected from the different spectrometries.

Recently, Nanba and Miura (2003) examined the alkali distribution in combining  $^{11}B$  and  $^{29}Si$  NMR data for  $RNa_2O \cdot B_2O_3 \cdot KSiO_2$  glasses, where the relative amounts of Na ions distributed to the structural units,  $f_{Na}$  were estimated from the simple assumptions. Firstly, it has been commonly accepted that oxygen atoms in  $BO_4$  units consisted entirely of BOs in  $B-O-B$  or  $B-O-Si$  bridges. In this case, the  $BO_4$  units possess a unit charge as  $[BO_{4/2}]^-$ . NBOs in  $\equiv Si-O^- \cdots Na^+$  and  $=B-O^- \cdots Na^+$  units also carry a negative charge of  $-1$ . Hence, the equivalent amount of  $Na^+$  ions is distributed to the  $[BO_{4/2}]^-$  units and NBOs for charge compensation. In an  $RNa_2O \cdot B_2O_3 \cdot KSiO_2$  glass, the amount of  $[BO_{4/2}]^-$  units is given by  $2N_4$ , where  $N_4$  is determined from  $^{11}B$  NMR.

Then, the fraction of Na ions distributed to the  $\text{BO}_4$  units,  $f_{\text{Na}}(\text{B4})$  is expected as

$$f_{\text{Na}}(\text{B4}) = 2N_4/2R = N_4/R. \quad (1)$$

It is generally accepted that Si atoms in alkali borosilicate glasses prefer tetrahedral sites, and they are classified into  $Q^n$  species which are associated with  $n$  BOs in Si–O–Si or Si–O–B bridges and  $(4 - n)$  NBOs in Si–O $\cdots$ Na units. In the  $R\text{Na}_2\text{O}\cdot\text{B}_2\text{O}_3\cdot K\text{SiO}_2$  glass, the total amount of NBOs in a  $Q^n$  species is expressed as  $f(Q^n)\times(4 - n)\times K$  by using the fraction of  $Q^n$  species,  $f(Q^n)$  determined from  $^{29}\text{Si}$  NMR. Consequently, the total fraction of Na ions compensating the negative charge of NBOs in  $\text{SiO}_4$  units,  $f_{\text{Na}}(\text{Si})$  can be estimated by

$$f_{\text{Na}}(\text{Si}) = \sum f(Q^n)\times(4 - n)\times K/2R. \quad (2)$$

It is finally expected that the residual Na ions are associated with the NBOs in  $\text{BO}_3$  units, because it has been commonly accepted that NBOs are preferentially formed in  $\text{BO}_3$  units rather than  $\text{BO}_4$  units (Scholze, 1991). Then, we obtain

$$f_{\text{Na}}(\text{B3}) = 1 - f_{\text{Na}}(\text{B4}) - f_{\text{Na}}(\text{Si}). \quad (3)$$

Even if NBOs are present in  $\text{BO}_4$  units, Eqn. 3 is valid. In such a case,  $f_{\text{Na}}(\text{B3})$  represents the fraction of Na ions distributed to the NBOs in borate ( $\text{BO}_3 + \text{BO}_4$ ) groups. In the alkali distribution estimated in this way (Nanba and Miura, 2003), it was found a strange result that  $f_{\text{Na}}(\text{B3})$  was negative at the small  $R$  region (see open markers in Fig. 4b), indicating that the amount of fourfold coordinated boron, B4 and/or the amount of NBO in  $\text{SiO}_4$  units were overestimated in the NMR analyses.

Such a contradiction in NMR has been already reported by Zhao et al. (2000). In barium borosilicate glass, different amounts of NBO were estimated from  $^{11}\text{B}$  and  $^{17}\text{O}$  NMR. It was concluded that the contradiction was due to the tricluster unit sharing one oxygen by three-tetrahedral  $\text{SiO}_4$  and  $\text{BO}_4$  units. For example, when two  $\text{BO}_4$  units are present in a tricluster  $(\text{O}_{3/2}\text{Si})\text{O}(\text{BO}_{3/2})_2$ , the charge of the tricluster unit is identified as  $-1$ , and hence only one Na is required to compensate its negative charge. As a result,  $f_{\text{Na}}(\text{B4})$  is overestimated.

On the other hand, Nanba and Miura (2003) proposed the following interpretation. When an NBO is formed in an  $\text{SiO}_4$  unit, the NBO in the  $\text{SiO}_4$  unit donates its lone pair electrons to the vacant  $\text{B}2p_z$  orbital in the neighboring  $\text{BO}_3$  unit, and the NBO turns into BO forming an Si–O–B4 bridge. The electronic delocalization through the B4–O bond is much less than that through the B3–O bond due to the lower  $\pi$ -bonding character of B4–O, and it is therefore expected that BOs in the Si–O–B4 bridges formed in this way

possess many electrons similar to the NBOs in Si–O–Na units and they have been assigned to NBO in Si-NMR. Bhasin et al. (1998) performed the deconvolution of  $^{29}\text{Si}$  MAS NMR spectra of ternary sodium borosilicate glasses, assuming the same chemical shifts of the  $Q^n$  species in binary sodium silicate glasses (Maekawa et al., 1991). The  $f_{\text{Na}}(\text{Si})$  given in the previous investigation (Nanba and Miura, 2003) was based on the  $Q^n$  fractions reported by Bhasin et al. (1998). If the interpretation by Nanba and Miura (2003) is appropriate, the  $^{29}\text{Si}$  chemical shifts of the  $Q^n$  species in borosilicate glasses should be revised. In practice, it was confirmed in aluminosilicates that the chemical shift of  $^{29}\text{Si}$  in  $Q^4$  species ranges over  $-86 \sim -110$  ppm and the chemical shift depends on the number of Al atoms at the second neighboring sites (Lippmaa et al., 1981). According to Maekawa et al. (1991),  $^{29}\text{Si}$  chemical shift is proportional to the optical basicity of glass matrix; in  $\text{Na}_2\text{O}$ – $\text{SiO}_2$  glasses,  $\text{Na}_2\text{O}$  addition results in the increase in basicity and  $^{29}\text{Si}$  shift to the smaller  $Q^n$  side. Based on the theoretical expression (Duffy and Ingram, 1976), the optical basicities of  $\text{B}_2\text{O}_3$ ,  $\text{SiO}_2$ , and  $\text{Al}_2\text{O}_3$  are estimated as 0.42, 0.48, and 0.59, respectively. It is hence expected that the addition of  $\text{Al}_2\text{O}_3$  into  $\text{SiO}_2$  results in the increase in basicity, and in the case of  $\text{B}_2\text{O}_3$  addition, however, the basicity decreases slightly. Actually, the  $^{29}\text{Si}$  chemical shifts of alkali-free borosilicate glasses are almost constant at  $-110$  ppm (Martin et al., 1992 ; Martens and Müller-Warmuth, 2000), which is the same as alkali-free silica glass. This is probably the reason why the assumption by Bhasin et al. (1998) has been accepted.

Recently, Du and Stebbins (2003) applied  $^{11}\text{B}$  and  $^{17}\text{O}$  triple quantum magic angle spinning (3QMAS) NMR to sodium borosilicate glasses, indicating the absence of NBOs in the glasses with low  $\text{Na}_2\text{O}$  content. This absence indicates the exclusive presence of  $Q^4$  species at small  $R$  regions, and hence the  $^{29}\text{Si}$  chemical shift in the NBO-free glasses should be attributed to Si–O–B bridges. In the alkali-free borosilicate glasses, tetrahedral borons are not present and  $^{29}\text{Si}$  peaks are commonly observed at around  $-110$  ppm (Martens and Müller-Warmuth, 2000). It is therefore supposed that not Si–O–B3 but Si–O–B4 bridges are responsible for the  $^{29}\text{Si}$  chemical shift in the small  $R$  regions. Furthermore, it was also noted that the presence of tricluster oxygens was negligible in the low alkali glasses, because tricluster oxygens were always accompanied by NBOs.

In the previous investigation (Nanba and Miura, 2003), the NMR data used were given by the different researchers ( $^{11}\text{B}$  NMR by Yun and Bray, 1978; Dell et al., 1983,

and  $^{29}\text{Si}$  MAS NMR by Bhasin et al., 1998). Therefore, NMR measurements using the same specimens were desired to confirm the contradiction in the alkali distribution. Then, in the present study,  $^{11}\text{B}$  and  $^{29}\text{Si}$  MAS NMR measurements were performed using the specimens prepared in the same manner, and the alkali distribution was reexamined according to the  $N_4$  and  $f(Q^n)$  data derived from the conventional procedures. Furthermore, molecular orbital theoretical calculations were performed to interpret the origin of the unexpected  $^{29}\text{Si}$  chemical shift in the sodium borosilicate glasses. As for aluminosilicates, ab initio studies by Xue and Kanzaki (1998, 1999) offer valuable insights for the NMR characteristics. In the case of borosilicates, however, little was published, and Lee et al. (2001) just discussed topological disorder and reactivity. Furthermore, little was discussed concerning the electronic states and chemical bonding character based on theoretical calculations. In the present study, the electronic states of borosilicate glass were also investigated on the basis of a cluster molecular orbital (MO) calculation for the purpose of obtaining the theoretical prediction of  $^{29}\text{Si}$  chemical shift. The cluster models were constructed based on a sodium borosilicate mineral, reedmergnerite  $\text{NaBSi}_3\text{O}_8$ . A structural group,  $\text{B}(\text{SiO}_4)_4$  in which a  $\text{BO}_4$  unit is surrounded by four  $\text{SiO}_4$  units, is present in the borosilicate mineral, and according to Yun and Bray (1978), the group is commonly present in borosilicate glasses. The alkali distribution model proposed by Dell et al. (1983), which has been most widely accepted, is based on this structural group. This mineral is also suitable for the present investigation. Neither  $\text{NBO}$  nor  $\text{BO}_3$  unit is present in the structure, but  $\text{Si-O-Si}$  bridges are present other than  $\text{B4-O-Si}$  bridges (Table 2b). Therefore, the electronic states and chemical bonding characters can be compared between the bridging bonds,  $\text{B4-O-Si}$  and  $\text{Si-O-Si}$  with the different atomic combinations.

## 2. EXPERIMENTAL

Glasses with the chemical composition,  $R\text{Na}_2\text{O}\cdot\text{B}_2\text{O}_3\cdot K\text{SiO}_2$  ( $K = 0.5$  and  $2.0$ ) were prepared by a conventional melt-quenching method. For Si-NMR measurements, 0.2 mol%  $\text{Fe}_2\text{O}_3$  was also added to the batches for reducing the spin lattice relaxation time. The 10-g batches were melted in a platinum crucible at  $1000^\circ\text{C}$  for 30 min to remove carbonates and were melted for 30 more min at  $1000 \sim 1300^\circ\text{C}$  with the lid of alumina, where the melts were stirred several times to obtain homogeneous specimens.

Postannealing was not done in order to avoid phase separation. Inductively coupled plasma analysis was done for some glasses prepared, and the compositional deviation of the cations was less than 5 atomic%.

NMR measurements were carried out at 7.05 T on a Varian <sup>UNITY</sup>INOVA300 spectrometer. The sample spinning speed at the magic angle to external field was 4.5 kHz. <sup>11</sup>B MAS NMR spectra were collected at 78.2 MHz with 1.0- $\mu$ s pulses and 1.0-s recycle delays, and <sup>29</sup>Si MAS NMR spectra were obtained at 59.6 MHz with 5.0- $\mu$ s pulses and 1.0-s recycle delays. The chemical shift standards used were BPO<sub>4</sub> for <sup>11</sup>B and poly (dimethyl siloxane) (PDMS) for <sup>29</sup>Si.

First-principle MO calculations were performed with the self-consistent-charge discrete-variational X $\alpha$  method (Adachi et al., 1978) using a Hartree-Fock-Slater approximation. Cluster models were constructed on the basis of the crystal structure of reedmergnerite, NaBSi<sub>3</sub>O<sub>8</sub> (Appleman and Clark, 1965). The clusters were embedded in a Madelung potential to reduce the termination effects. The atomic orbitals used in the calculations are Si 1s–3d, O 1s–2p, and Na 1s–3d. Chemical bonding character was estimated from net charge and bond overlap population on the basis of the Mulliken population analysis (Mulliken, 1955). In our experience for the silicate crystals (Nanba et al., 2003), atoms near the cluster surface have a tendency to possess unrealistic charges even in applying Madelung potentials, and hence for evaluating the electronic state of an atom, it should be surrounded by at least two layers of SiO<sub>4</sub> tetrahedra. In reedmergnerite crystal, there are 13 distinct crystallographic sites. If a cluster model were constructed in which each site had the second neighboring SiO<sub>4</sub> or BO<sub>4</sub> tetrahedra, the cluster would become too huge to perform the MO calculation. Then, 13 cluster models were constructed in which the atoms at the respective crystallographic sites were located at the center of the clusters and the central atoms were covered by at least two layers of SiO<sub>4</sub> or BO<sub>4</sub> tetrahedra. The radius of the clusters is 0.75 nm for Na (central atom), 0.7 nm for B and Si, and 0.6 nm for O. The B-centered cluster model, (Na<sub>9</sub>B<sub>5</sub>Si<sub>17</sub>O<sub>64</sub>)<sup>36-</sup> is illustrated in Figure 1. The population analyses were done only for the central atom and the bonds including the central atom.

### 3. RESULTS

#### 3.1. NMR Spectrometry and Alkali Distribution

Figure 2 shows  $^{11}\text{B}$  and  $^{29}\text{Si}$  MAS NMR spectra for  $R\text{Na}_2\text{O}\cdot\text{B}_2\text{O}_3\cdot K\text{SiO}_2$  ( $K = 0.5$ ) glasses. In  $^{11}\text{B}$  MAS NMR spectra (Fig. 2a), the symmetric sharp peak at around 5 ppm is attributed to B4 in  $\text{BO}_4$  unit, and the asymmetric broad peak at  $20 \sim -20$  ppm is assigned to B3 in  $\text{BO}_3$  unit. In  $^{29}\text{Si}$  MAS NMR spectra (Fig. 2b), the peak shifts to the higher relative frequency side with increasing  $R$ , indicating the increase of NBO in  $\text{SiO}_4$  unit according to the conventional interpretation. The spectra were deconvoluted into the structural components,  $\text{B}_n$  and  $\text{Q}^n$  species (Fig. 3), obtaining  $N_4$  and  $\text{Q}^n$  distribution. In the deconvolution of  $^{29}\text{Si}$  MAS NMR spectra, the position of the  $\text{Q}^n$  components was settled on the basis of the results for sodium silicate glasses (Maekawa et al., 1991). The  $N_4$  and  $\text{Q}^n$  distribution obtained (Table 1) have margins of error of 3% and 5%, respectively.

Alkali distribution estimated from Eqns. 1–3 is shown in Table 1 and Figure 4. In the glasses at  $K = 0.5$ ,  $f_{\text{Na}}(\text{B4})$  exceeds 100% at  $R = 0.2$  and  $0.4$ , which probably resulted from the compositional deviation. During the melting process,  $\text{B}_2\text{O}_3$  volatilizes slightly, and the relative amount of  $\text{Na}_2\text{O}$  increases. Hence, the actual  $\text{Na}_2\text{O}$  content,  $R$ , in the products should be larger than the nominal content. Therefore, the  $f_{\text{Na}}(\text{B4})$  values at the nominal compositions should be smaller than the observation.  $f_{\text{Na}}(\text{B4})$  is given by the division of  $N_4$  by  $R$ , and it is hence expected that  $f_{\text{Na}}(\text{B4})$  at smaller  $R$  region has larger numerical error (10% at a maximum) due to the compositional deviation. In the glasses indicating  $f_{\text{Na}}(\text{B4}) > 100\%$ , the actual  $R$  must be 0.21 and 0.42, expecting  $f_{\text{Na}}(\text{B4}) = 100\%$ .

As shown in Figure 4b by the open markers, the alkali distributions were also estimated from the NMR data reported by Dell et al. (1983), Yun and Bray (1978), and Bhasin et al. (1998). The agreement in  $f_{\text{Na}}(\text{B4})$  between the present and previous results is a satisfactory level. The  $f_{\text{Na}}(\text{Si})$  data are also consistent, with an exception at  $R = 1.0$ . In both  $K$ -series,  $f_{\text{Na}}(\text{B3})$  shows negative value at small  $R$  regions. As mentioned,  $f_{\text{Na}}(\text{B4})$  is overestimated in observation due to the compositional deviation, and it is also the case in  $f_{\text{Na}}(\text{Si})$ . However,  $f_{\text{Na}}(\text{B3})$  values smaller than  $-10\%$  are out of the margin of error. As also described, the glasses with  $f_{\text{Na}}(\text{B4}) > 100\%$  should be 100% in the actual  $f_{\text{Na}}(\text{B4})$  value, which means that  $f_{\text{Na}}(\text{Si})$  as well as  $f_{\text{Na}}(\text{B3})$  should be 0% in these glasses. As shown in Table 1 and Figure 4a, however,  $f_{\text{Na}}(\text{Si})$  in these glasses is much larger than 0%, that is,  $f_{\text{Na}}(\text{Si}) = 9\%$  and  $16\%$  at  $R = 0.2$  and  $0.4$ , respectively. As shown in Figure

3b, the  $^{29}\text{Si}$  MAS NMR spectrum at  $R = 0.2$  consists of two components located at  $-105$  and  $-90$  ppm, which have been conventionally assigned to  $\text{Q}^4$  and  $\text{Q}^3$  species, respectively. In sodium silicate glasses, the chemical shift of  $^{29}\text{Si}$  ranges over  $-96 \sim -110$  ppm for  $\text{Q}^4$  and  $-85 \sim -92$  ppm for  $\text{Q}^3$  species (Maekawa et al., 1991). Therefore, it is tentatively concluded from Figure 3b that a measurable amount of NBO is present in the glass. This conclusion obtained from  $^{29}\text{Si}$ -NMR is, however, inconsistent with the conclusion from  $^{11}\text{B}$  NMR, that is, the amount of NBO is negligible from  $^{11}\text{B}$  NMR and not negligible from  $^{29}\text{Si}$ -NMR. It should be emphasized that the contradiction between  $^{11}\text{B}$  and  $^{29}\text{Si}$ -NMR is confirmed even in the glass specimens prepared in the same way. It is also noted that the contradiction is significant only when the  $-90$  ppm component is attributable to the  $\text{Q}^3$  species even in the borosilicate glasses.

### 3.2. Atomic Charge

It is commonly accepted that atomic charge is different between BO and NBO. If the chemical bonding character is completely ionic, both BO and NBO carry the same charge of  $-2$ . According to the formal charge assuming 100% covalency, however, the formal charge of NBO becomes  $-1$ , while BO is neutral. In practice, their charges are intermediate between  $-2$  and  $0$ , and it is expected that NBO possesses more electrons than BO. Then, the net charge,  $Z_n$  of oxygen atoms was examined from MO calculations (Table 2a and Fig. 5a).

As expected, NBO in sodium disilicate ( $\text{Na}_2\text{Si}_2\text{O}_5$ ) has smaller net charge (higher electronic population) than BO (Nanba et al., 2003). In reedmergnerite ( $\text{NaBSi}_3\text{O}_8$ ), there are eight oxygen sites; four sites in the B–O–Si bridge and another four sites in Si–O–Si, indicating broad  $Z_n$  distribution. The average  $Z_n(\text{O})$  of the borosilicate is higher than that of the silicate. Furthermore, the average  $Z_n(\text{O})$  in the B–O–Si bridge is slightly higher than that in the Si–O–Si bridge in the borosilicate. This result is disappointing, compared to the original expectation that some oxygens in the B–O–Si bridge possess higher electronic population than those in the Si–O–Si bridge.

The net charge of silicon,  $Z_n(\text{Si})$ , is also shown in Figure 5b. In the sodium silicates,  $Z_n(\text{Si})$  decreases with increasing the number of NBO in  $\text{SiO}_4$  units (in the order of  $\text{Q}^4$ ,  $\text{Q}^3$ , and  $\text{Q}^2$ ). In the sodium borosilicate,  $Z_n(\text{Si})$  is distributed between 2.05 and 1.95. It is noted that silicons in the sodium borosilicate have closer charge of  $\text{Q}^3$  silicon rather than

Q<sup>4</sup> silicon in the sodium silicates.

### 3.3. Chemical Shift in Energy Level

According to Grunthaner and Grunthaner (1986), the chemical shift in NMR is proportional to the chemical shift in XPS, that is, the energy shift in the core-level atomic orbitals. As is generally known, BO and NBO give different O1s binding energy in XPS. Then, O1s and Si2p orbital energies were examined (Table 2a). However, the absolute value of the orbital energies is not given in the MO calculation used in the present study, and hence the orbital energies between the different clusters are not compared directly. Next, the energy correction was done as follows. A cluster in which O(1) was the central atom (designated as O(1) cluster) was chosen for the energy correction, and the central O(1) and its nearest neighbors, B and Si(1) in the O(1) cluster were used as the energy standards; O(1)1s = -504.4 eV, B1s = -172.9 eV and Si(1)2s = -133.7 eV. Si(1)2p was not chosen as the energy standard, because it split into three levels. As listed in Table 2b, B has another three ligand oxygens, O(3), O(5), and O(7). Then, the orbital energies in O(3), O(5), and O(7) clusters were corrected as B1s of borons bound to the central oxygens to be -172.9 eV. The orbital energies of O(4), O(6), and O(8) clusters including Si(1) as the nearest neighbor of the central oxygens were also corrected using Si(1)2s. The orbital energies of the O(2) cluster were corrected by Si(2)2s averaging over the clusters, O(3), O(6), and O(8). Finally, the Si2p orbital energies of Si(1), Si(2) and Si(3) were estimated with the average energies among the oxygen-centered clusters.

Figure 6 shows the electronic density of states (DOS) of the atomic orbitals, O1s and Si2p. The partial density of states (PDOS) of oxygens in the Si–O–Si bridge is situated at a lower energy side than that in the B–O–Si bridge, from which it is generally interpreted that oxygens in the Si–O–Si bridge have smaller electronic population, that is, less negative charge, than those in the B–O–Si bridge. The electronic population expected is inconsistent with the results of net charge indicated in Table 2a and Figure 5a.

The shape of total DOS of O1s (Fig. 6a) is asymmetric, which is due to the outlying O(5) component. In Figure 6a, the O1s energies of BO and NBO in sodium disilicate (Nanba et al., 2003) are also shown as vertical lines. It is noteworthy that the energy

difference between BO and NBO in the silicate is almost the same as the difference between the average in Si–O–Si and O(5) in B–O–Si. Supposing that O1s XPS spectrum were measured, the shoulder due to O(5), if present, would be assigned as NBO.

Figure 6b shows DOS of Si2p. As mentioned, Si2p splits into three distinct levels in MO calculation. From the average values listed in Table 2a, PDOS values shown in Figure 6b were obtained. In the case of net charge, three silicons are at even intervals (Fig. 5b). In DOS, however, Si(1) and Si(2) are located at almost the same energy, but Si(3) is ~0.7 eV away from the other ones. It is notable that the energy difference is almost a half of the difference between Q<sup>4</sup> and Q<sup>3</sup> silicons. It is therefore expected that Si(3) gives a peak at higher relative frequency side in <sup>29</sup>Si-NMR.

Geisinger et al. (1988) reported the <sup>29</sup>Si MAS NMR data of reedmergnerite. Three well-resolved peaks are observed at –95.5, –98.4, and –107.1 ppm, and the chemical shifts are within the region of Q<sup>4</sup> silicon (–96 ~ –110 ppm) in sodium silicate glasses (Maekawa et al., 1991). The <sup>29</sup>Si peak at –95.5 ppm is attributable to Si(3), because similarities between Si(3) in reedmergnerite and Q<sup>3</sup> silicon in sodium disilicate are found both in net charge and Si2p orbital energy obtained from the MO calculations. Additionally, O(5) which shows the highest O1s energy is bound to Si(3) (Table 2b). The other peaks at –98.4 and –107.1 ppm probably originate in Si(2) and Si(1), respectively. If Si2p energy of Si(2) estimated from the MO calculations were much closer to that of Si(3) instead of Si(1), this assignment would be more reliable.

## 4. DISCUSSION

### 4.1. Chemical Bonding Character

It was found in the present MO calculations that Si(3) in reedmergnerite had higher electronic population and higher Si2p energy than the other silicons, and it was also suggested that the electronic state of Si(3) was quite similar to that of Q<sup>3</sup> silicon in sodium silicate. Then, chemical bonding character was examined based on the bond overlap population (BOP) for clarifying the origin of the specific properties of Si(3). The physical meaning of BOP is the population of electrons shared between two atoms (Mulliken, 1955), and it is often associated with bond order and bond modulus.

Figure 7 shows BOPs in the borosilicate crystal together with the data for the silicate and borate crystals. It is noted that Si–O bonds show different BOP between Si–O–Si and Si–O–B4 bridges, and B4–O bond shows smaller BOP compared with the Si–O bonds. B4–O bond in the borate crystal also shows smaller BOP than the other B–O bonds, and BOP in the B4–O–B4 bridge is, however, almost the same with that in the B3–O–B3 bridge. The relation of BOP in magnitude between the bonds, B4–O and B3–O in a B4–O–B3 bridge is quite similar to the relation between the bonds, B4–O and Si–O in the B4–O–Si bridges. In the heterogeneous combinations, such as B4–O–Si and B4–O–B3 bridges, B4–O bonds always show much smaller BOP (~0.5), while the opponent Si–O and B3–O bonds indicate higher BOP (~0.7) as compared with the homogeneous combinations, Si–O–Si, B3–O–B3 and B4–O–B4 (~0.6). It is also notable that the homogeneous combinations indicate almost the same BOP (~0.6) even in the different crystals. It is therefore concluded that electrons are evenly distributed between the bonds in the homogeneous combinations, and in the heterogeneous combinations, such as Si–O–B4 and B3–O–B4 bridges, however, the electron distribution is unequal and many electrons are localized on Si–O and B3–O bonds. Moreover, the difference in BOP between Si–O and B4–O bonds in Si–O–B4 bridges (~0.2) is close to the difference between Si–BO and Si–NBO bonds in the silicate crystal. Certainly, the absolute value of BOP of Si–O in Si–O–B4 bridges (0.72) is much less than that of Si–NBO (0.84). In reedmergnerite, Si(3) has two B4 borons as the second nearest neighbors, whereas Si(1) and Si(2) have one second-neighboring B4. The difference in BOP indicates means that the electronic population around Si(3) is higher than Si(1) and Si(2), and it is probably the reason for the higher net charge and Si2p energy of Si(3).

#### **4.2. Interpretation of the –90 ppm Component in <sup>29</sup>Si-NMR**

The contradiction in alkali distribution was confirmed from the experiments; <sup>11</sup>B NMR suggests that Na ions are exclusively distributed to BO<sub>4</sub> units and NBO is not present in the low alkali content glasses, whereas <sup>29</sup>Si-NMR indicates that the negligible amount of Na ions are distributed to SiO<sub>4</sub> units forming NBOs in the glasses. However, this conclusion is based on the two hypotheses. It has been assumed that the –90 ppm

component observed in  $^{29}\text{Si}$  NMR (Fig. 3b) was attributable to the  $\text{Q}^3$  unit even in the case of borosilicate glasses. As for the  $\text{Q}^4$  species in aluminosilicates, the  $^{29}\text{Si}$  NMR peak shifts to the higher relative frequency side with increasing the number of second neighboring Al, and the  $^{29}\text{Si}$  chemical shift of Si surrounded by three Al is around  $-90$  ppm (Lippmaa et al., 1981), which overlaps with the region for the  $\text{Q}^3$  species in sodium silicate glasses (Maekawa et al., 1991). As mentioned, the situation in aluminosilicates is apparently similar to the borosilicate glass. According to the basicity concept proposed by Duffy and Ingram (1976), the basicities of oxygens in Si–O–Si, Si–O–B4 and Si–O–Al bridges are estimated as 0.48, 0.52, and 0.59, respectively. If  $^{29}\text{Si}$ -NMR chemical shift is proportional to the basicity of surrounding oxygens, the chemical shift in borosilicates should be much smaller than that in aluminosilicates. In practice, however, the chemical shift is affected by other factors, such as bond strength and bond angle of Si–O–T bridges (Stebbins, 1995). In any case, the results obtained in this paper suggest that the  $-90$  ppm component in  $^{29}\text{Si}$  NMR should be assigned not only to  $\text{Q}^3$  species with one NBO but also to  $\text{Q}^4$  species associated with abundant B4 as second neighbors. Direct estimation of the NMR parameters, such as the theoretical elucidation by Xue and Kanzaki (1998, 1999) should be required for further discussion.

Another hypothesis is that a  $\text{BO}_4$  unit possesses a negative charge of  $-1$ , and one Na ion is distributed around the  $\text{BO}_4$  unit as a charge compensator. This hypothesis is valid, when all four oxygens are usual BOs in the bridges, such as B–O–B and B–O–Si. However, if tricluster oxygen such as B4–O– $\text{M}_2$  ( $\text{M} = \text{Si}$  or B4) is present, the negative charge of the  $\text{BO}_4$  unit is reduced. As mentioned, the charge of a tricluster,  $(\text{O}_{3/2}\text{Si})\text{O}(\text{BO}_{3/2})_2$  including two  $\text{BO}_4$  units is  $-1$ , and hence only one Na is required for the charge neutrality. The atoms left over in this way, Na and  $\frac{1}{2}\text{O}$  are used for the formation of NBO elsewhere in the material. Zhao et al. (2000) proposed this model to interpret the contradiction between  $^{11}\text{B}$  and  $^{17}\text{O}$  NMR in barium borosilicate glasses, and they also stated that the experimental observation of the tricluster oxygens is quite difficult even in  $^{17}\text{O}$  NMR. Lee et al. (2001) examined the stability of a tricluster based on the theoretical calculations, inferring small fractions of the tricluster. According to the latest  $^{17}\text{O}$  3QMAS NMR analyses for sodium borosilicate glasses (Du and Stebbins, 2003), no NBO peaks were observed in the glasses with low  $\text{Na}_2\text{O}$  content, suggesting that the effects due to the tricluster oxygens and NBOs on the  $^{29}\text{Si}$  chemical shifts were negligible in the low  $\text{Na}_2\text{O}$  glasses.

At this moment, these hypotheses are not denied or confirmed. A tentative conclusion should be drawn as follows. The triclusters and NBOs derived from the triclusters are present in borosilicate glass but not so abundant as to compensate the fictitious  $Q^3$  component at  $-90$  ppm in  $^{29}\text{Si}$  NMR spectra on their own. Another compensator for the  $-90$  ppm component is BOs in B4–O–Si bridges which are in a similar electronic state to NBOs. In the NBO-free glasses ( $K = 0.5$ ,  $R = 0.2$  and  $0.4$ ), the amount of the fictitious NBOs per Si is estimated as  $0.07$  and  $0.26$  at  $R = 0.2$  and  $0.4$ , respectively. If the  $Q^4$  silicons associated with two tetrahedral borons are assigned as the fictitious  $Q^3$  silicons, the amount of tetrahedral borons next to the fictitious  $Q^3$  silicons is expected as  $0.14$  ( $0.07 \times 2$ ) and  $0.52$  at the maximum, which is much less than the total amount of tetrahedral borons present in the glasses,  $0.85$  ( $2 \times 0.21 / 0.5$ ) and  $1.68$  at  $R = 0.2$  and  $0.4$ , respectively. Furthermore, according to Du and Stebbins (2003), tetrahedral borons are preferentially associated with silicons to form B4–O–Si bridges. It is therefore concluded that there are enough tetrahedral borons to compensate the  $-90$  ppm component.

Before beginning MO calculations, it was expected that O(1) in reedmergnerite would show a similar character to NBO because it had two neighboring Na (Table 2b). As shown in Table 2a and Figure 6a, however, O(5) showed the highest O1s energy which was close to NBO in sodium silicate. As theoretically elucidated by Xue and Kanzaki (1998, 1999), the chemical shifts in  $^{29}\text{Si}$  and  $^{17}\text{O}$  NMR depend on the bond angle of the Si–O–T bridge ( $T = \text{Si}, \text{Al}$ ); the chemical shifts commonly move to the higher relative frequency side with decreasing the bond angle. Among B–O–Si bridges in reedmergnerite, the B–O(5)–Si(3) bridge is narrowest (Table 2b). The narrow bond angle is probably the reason for the distinctive characteristics in O(5) and Si(3). It is finally expected that some B4–O–Si bridges in borosilicate glass are in a narrow bond angle, and Si atoms in the narrow B4–O–Si bridges appear in the  $-90$  ppm component, which has been attributed to  $Q^3$  species according to the conventional assignments.

## 5. CONCLUSIONS

$^{11}\text{B}$  and  $^{29}\text{Si}$  MAS NMR spectra were measured for  $\text{Na}_2\text{O}-\text{B}_2\text{O}_3-\text{SiO}_2$  glasses. For the glasses with low  $\text{Na}_2\text{O}$  content,  $^{11}\text{B}$  NMR suggested that Na ions were exclusively distributed to borate groups forming  $\text{BO}_4$  units, whereas a  $-90$  ppm component was

extracted from  $^{29}\text{Si}$ -NMR spectra, which had so far been attributed to  $\text{Q}^3$  species in accordance with the conventional assignments. To clarify the origin of the fictitious  $\text{Q}^3$  component in  $^{29}\text{Si}$ -NMR, MO calculations were performed to evaluate the electronic states of Si and O atoms, where cluster models were constructed on the basis of a borosilicate crystal, reedmergnerite  $\text{NaBSi}_3\text{O}_8$ . Among the three Si sites in the borosilicate crystal, Si(3) which was  $\text{Q}^4$  species in the conventional notation was similar in net charge and Si2p energy to  $\text{Q}^3$  species in sodium silicates. The results led to a conclusion that the  $\text{Q}^4$  species which were in a similar environment to Si(3) were responsible for the fictitious  $\text{Q}^3$  species in  $^{29}\text{Si}$ -NMR spectra. There still remained a possibility that the triclusters such as  $(\text{O}_{3/2}\text{Si})\text{O}(\text{BO}_{3/2})_2$  were present in borosilicate glasses, but the triclusters were probably not so abundant to contribute to the  $-90$  ppm component.

The chemical bonding character was also estimated on the basis of the bond overlap population. It was found that electrons were unequally distributed around oxygens in Si–O–B4 bridges, and many electrons were localized on Si–O bonds, suggesting that the  $\text{Q}^4$  species associated with abundant B4 atoms as the second neighbors were responsible for the fictitious  $\text{Q}^3$  species. It was also suggested that Si–O–B4 bridges with narrow bond angle contributed to the  $-90$  ppm component in  $^{29}\text{Si}$ -NMR spectra. In any case, theoretical predictions of the NMR parameters are required to clarify the chemical shifts of the  $\text{Q}^n$  species in borosilicates.

*Acknowledgments*—The authors would like to thank Claudia Romano and three anonymous reviewers whose comments improved the manuscript. Also, the authors acknowledge helpful comments and suggestions by Jonathan F. Stebbins, Xianyu Xue, and Masami Kanzaki.

## REFERENCES

- Adachi H., Tsukada M., and Satoko C. (1978) Discrete variational  $X\alpha$  cluster calculations. I. Application to metal clusters. *J. Phys. Soc. Jpn.* **45**, 875–883.
- Appleman D. E. and Clark J. R. (1965) Crystal structure of reedmergnerite, a boron albite, and its relation to feldspar crystal chemistry. *Am. Mineral.* **50**, 1827–1850.
- Bhasin G., Bhatnagar A., Bhowmik S., Stehle C., Affatigato M., Feller S., MacKenzie J., and Martin S. (1998) Short range order in sodium borosilicate glasses obtained via deconvolution of  $^{29}\text{Si}$  MAS NMR spectra. *Phys. Chem. Glasses* **39**, 269–274.
- Dell W. J., Bray P. J., and Xiao S. Z. (1983)  $^{11}\text{B}$  NMR studies and structural modeling of  $\text{Na}_2\text{O}-\text{B}_2\text{O}_3-\text{SiO}_2$  glasses of high soda content. *J. Non-Cryst. Solids* **58**, 1–16.
- Du L.-S. and Stebbins J. F. (2003) Nature of silicon-boron mixing in sodium borosilicate glasses: A high-resolution  $^{11}\text{B}$  and  $^{17}\text{O}$  NMR study. *J. Phys. Chem. B* **107**, 10063–10076.
- Duffy J. A. and Ingram M. D. (1976) An interpretation of glass chemistry in terms of the optical basicity concept. *J. Non-Cryst. Solids* **21**, 373–410.
- Geisinger K. L., Oestrike R., Navrotsky A., Turner G. L., and Kirkpatrick R. J. (1988) Thermochemistry and structure of glasses along the join  $\text{NaAlSi}_3\text{O}_8$ -  $\text{NaBSi}_3\text{O}_8$ . *Geochim. Cosmochim. Acta* **52**, 2405–2414.
- Grunthaner F. J. and Grunthaner P. J. (1986) Chemical and electronic structure of the  $\text{SiO}_2/\text{Si}$  interface. *Mater. Sci. Rep.* **1**, 65–160.
- Lee S. K., Musgrave C. B., Zhao P., and Stebbins J. F. (2001) Topological disorder and reactivity of borosilicate glasses: Quantum chemical calculations and  $^{17}\text{O}$  and  $^{11}\text{B}$  NMR study. *J. Phys. Chem. B* **105**, 12583–12595.
- Lippmaa E., Maegi M., Samoson A., Tarmak M., and Engelhardt G. (1981) Investigation of the structure of zeolites by solid-state high-resolution  $^{29}\text{Si}$  NMR spectroscopy. *J. Am. Chem. Soc.* **103**, 4992–4996.
- MacKenzie J. W., Bhatnagar A., Bain D., Bhowmik S., Parameswar C., Budhwani K., Feller S. A., Royle M. L., and Martin S. W. (1994)  $^{29}\text{Si}$  MAS-NMR study of the short range order in alkali borosilicate glasses. *J. Non-Cryst. Solids* **177**, 269–276.
- Maekawa H., Maekawa T., Kawamura K., and Yokokawa T. (1991) The structural groups of alkali silicate glasses determined from  $^{29}\text{Si}$  MAS-NMR. *J. Non-Cryst. Solids* **127**, 53–64.

- Martens R. and Müller-Warmuth W. (2000) Structural groups and their mixing in borosilicate glasses of various compositions – an NMR study. *J. Non-Cryst. Solids* **265**, 167–175.
- Martin S.W., Bain D., Budhwani K., and Feller S. (1992)  $^{29}\text{Si}$  MAS-NMR study of the short-range order in lithium borosilicate glasses. *J. Am. Ceram. Soc.* **75**, 1117–1122.
- Miura Y., Kusano H., Nanba T., and Matsumoto S. (2001) X-ray photoelectron spectroscopy of sodium borosilicate glasses. *J. Non-Cryst. Solids* **290**, 1–14.
- Mulliken R. S. (1955) Electronic populations analysis on LCAO-MO molecular wave functions. I & II. *J. Chem. Phys.* **23**, 1833–1846.
- Nanba T., Hagiwara T., and Miura Y. (2003) Chemical bonding state of sodium silicates. *Adv. Quantum Chem.* **42**, 187–198.
- Nanba T. and Miura Y. (2003) Alkali distribution in borosilicate glasses. *Phys. Chem. Glasses* **44**, 244–248.
- Scholze H. (1991) Glass - Nature, Structure and Properties. Springer-Verlag, New York, pp. 128–149.
- Stebbins J. F. (1995) Dynamics and structure of silicate and oxide melts: Nuclear magnetic resonance studies. In *Rev. in Mineralogy*, Vol. 32(eds. J. F. Stebbins, P. F. McMillan and D. B. Dingwell), pp. 191–246, Mineralogical Society of America.
- Xue X. and Kanzaki M. (1998) Correlations between  $^{29}\text{Si}$ ,  $^{17}\text{O}$  and  $^1\text{H}$  NMR properties and local structures in silicates: An ab initio calculation. *Phys. Chem. Minerals* **26**, 14–30.
- Xue X. and Kanzaki M. (1999) NMR characteristics of possible oxygen sites in aluminosilicate glasses and melts: An ab initio study. *J. Phys. Chem. B* **103**, 10816–10830.
- Yun Y. H. and Bray B. J. (1978) Nuclear magnetic resonance studies of the glasses in the system  $\text{Na}_2\text{O}-\text{B}_2\text{O}_3-\text{SiO}_2$ . *J. Non-Cryst. Solids* **27**, 363–380.
- Zhao P., Kroeker S., and Stebbins J. F. (2000) Non-bridging oxygen sites in barium borosilicate glasses: Results from  $^{11}\text{B}$  and  $^{17}\text{O}$  NMR. *J. Non-Cryst. Solids* **276**, 122–131.
- Zhong J., Wu X., Liu M. L., and Bray P. J. (1988) Structural modeling of lithium borosilicate glasses via NMR studies. *J. Non-Cryst. Solids* **107**, 81–87.

## Tables

Table 1. Fraction of 4-fold boron,  $N_4$  obtained from  $^{11}\text{B}$  MAS NMR,  $Q^n$  distribution from  $^{29}\text{Si}$  MAS NMR, and alkali distribution from Eqns. 1~3 for  $R\text{Na}_2\text{O}\cdot\text{B}_2\text{O}_3\cdot\text{KSiO}_2$  glasses.

Composition		$N_4$ (%)	$Q^n$ distribution (%)				Alkali distribution (%)		
$K$	$R$		$f(Q^4)$	$f(Q^3)$	$f(Q^2)$	$f(Q^1)$	$f_{\text{Na}}(\text{B4})$	$f_{\text{Na}}(\text{B3})$	$f_{\text{Na}}(\text{Si})$
0.5	0	0	100	0	0	0			
	0.2	21	93	7	0	0	107	-16	9
	0.4	42	74	26	0	0	105	-21	16
	0.6	50	67	28	5	0	83	1	16
	0.8	49	16	68	16	0	61	8	31
	1.0	47	3	46	49	3	47	15	38
	1.2	39	0	28	69	3	33	31	36
2.0	0.45	38	86	14	0	0	84	-17	32
	0.6	45	78	22	0	0	75	-12	37
	1.0	60	57	43	0	0	60	-3	43
	2.0	45	0	71	29	0	23	13	64
	2.5	33	0	41	54	5	13	21	66
	3.0	22	0	31	53	16	7	31	62

Table 2. Summary of the MO calculations and local structures around oxygen.

(a) Net charge  $Z_n$ , and atomic orbital energy  $E_{AO}$  (O1s, B1s, Si2p and Na1s)

Site	$Z_n$	$E_{AO}$ (eV)	Site	$Z_n$	$E_{AO}$ (eV)
O(1)	-0.990	-504.38	B	1.399	-172.92
O(2)	-1.018	-505.03	Si(1)	2.034	-91.15
O(3)	-1.030	-504.19	Si(2)	1.985	-90.96
O(4)	-1.004	-505.30	Si(3)	1.935	-90.35
O(5)	-1.013	-503.35	Na	0.861	-1022.02
O(6)	-1.061	-504.62			
O(7)	-1.042	-504.29			
O(8)	-1.051	-505.31			

(b) Bond distance  $r$ , bond overlap population BOP, and bond angle  $\angle(\text{B,Si})\text{-O-Si}$

	Bond	$r$ (nm)	BOP	$\angle$ ( $^\circ$ )
O(1)	-B	0.1478	0.480	} 143.1
	-Si(1)	0.1595	0.751	
	-Na	0.2464	0.048	
	-Na	0.2498	0.030	
O(2)	-Si(2)	0.1636	0.652	} 128.4
	-Si(3)	0.1648	0.598	
	-Na	0.2412	0.037	
O(3)	-B	0.1477	0.481	} 140.7
	-Si(2)	0.1592	0.738	
	-Na	0.2410	0.024	
O(4)	-Si(1)	0.1611	0.676	} 158.2
	-Si(3)	0.1626	0.642	
O(5)	-B	0.1445	0.538	} 124.7
	-Si(3)	0.1612	0.718	
O(6)	-Si(1)	0.1625	0.625	} 135.8
	-Si(2)	0.1630	0.602	
	-Na	0.2817	0.016	
O(7)	-B	0.1473	0.501	} 135.4
	-Si(3)	0.1614	0.685	
	-Na	0.2382	0.027	
O(8)	-Si(1)	0.1623	0.633	} 146.3
	-Si(2)	0.1613	0.616	
	-Na	0.2862	0.012	

## Figure Captions

Fig. 1. An example of the cluster models. Boron-centered ( $\text{Na}_9\text{B}_5\text{Si}_{17}\text{O}_{64}$ )<sup>36-</sup> cluster. The symbols with numbers, Si1~3 and O1~8 represent the crystallographic sites in reedmergnerite (Appleman and Clark, 1965).

Fig. 2. <sup>11</sup>B and <sup>29</sup>Si MAS NMR spectra at 7.05 T for  $R\text{Na}_2\text{O}\cdot\text{B}_2\text{O}_3\cdot K\text{SiO}_2$  glasses ( $K = 0.5$ ). The vertical lines indicate the general position of <sup>29</sup>Si chemical shifts in sodium silicate glasses (Maekawa et al., 1991).

Fig. 3. Examples of spectral deconvolution of <sup>11</sup>B and <sup>29</sup>Si MAS NMR spectra for an  $R\text{Na}_2\text{O}\cdot\text{B}_2\text{O}_3\cdot K\text{SiO}_2$  glass ( $R = 0.2, K = 0.5$ ). The simulated components and total curves are shown by dotted lines. The fitting parameters used in the spectral simulation are also shown (QCC: quadrupolar coupling constant,  $\delta$ : isotropic chemical shift,  $\eta$ : asymmetry parameter).

Fig. 4. Relative amount of Na ions distributed to  $\text{BO}_4$  units,  $f_{\text{Na}}(\text{B4})$ , NBO in  $\text{BO}_3$  units,  $f_{\text{Na}}(\text{B3})$ , and NBO in  $\text{SiO}_4$  units,  $f_{\text{Na}}(\text{Si})$  for  $R\text{Na}_2\text{O}\cdot\text{B}_2\text{O}_3\cdot K\text{SiO}_2$  glasses. Closed markers: present study, open markers: estimation from the NMR data given by Dell et al. (1983), Yun and Bray (1978), and Bhasin et al. (1998).

Fig. 5. Net charge,  $Z_n$  obtained from the MO calculations. \* Nanba et al. (2003).

Fig. 6. Density of states (DOS) of the atomic orbitals obtained from the MO calculations. Curves were obtained assuming a gaussian profile with a 1.0-eV full width at the half maximum. The vertical lines are the energy levels in sodium silicates (Nanba et al., 2003).

Fig. 7. Bond overlap population, BOP, obtained from the MO calculations. For instance, B4-O(-Si) represents BOP of B4-O bond in B4-O-Si bridge. Cross markers in  $\text{NaBSi}_3\text{O}_8$  indicate the average of open markers. \*1: Nanba et al. (2003); \*2: unpublished data.

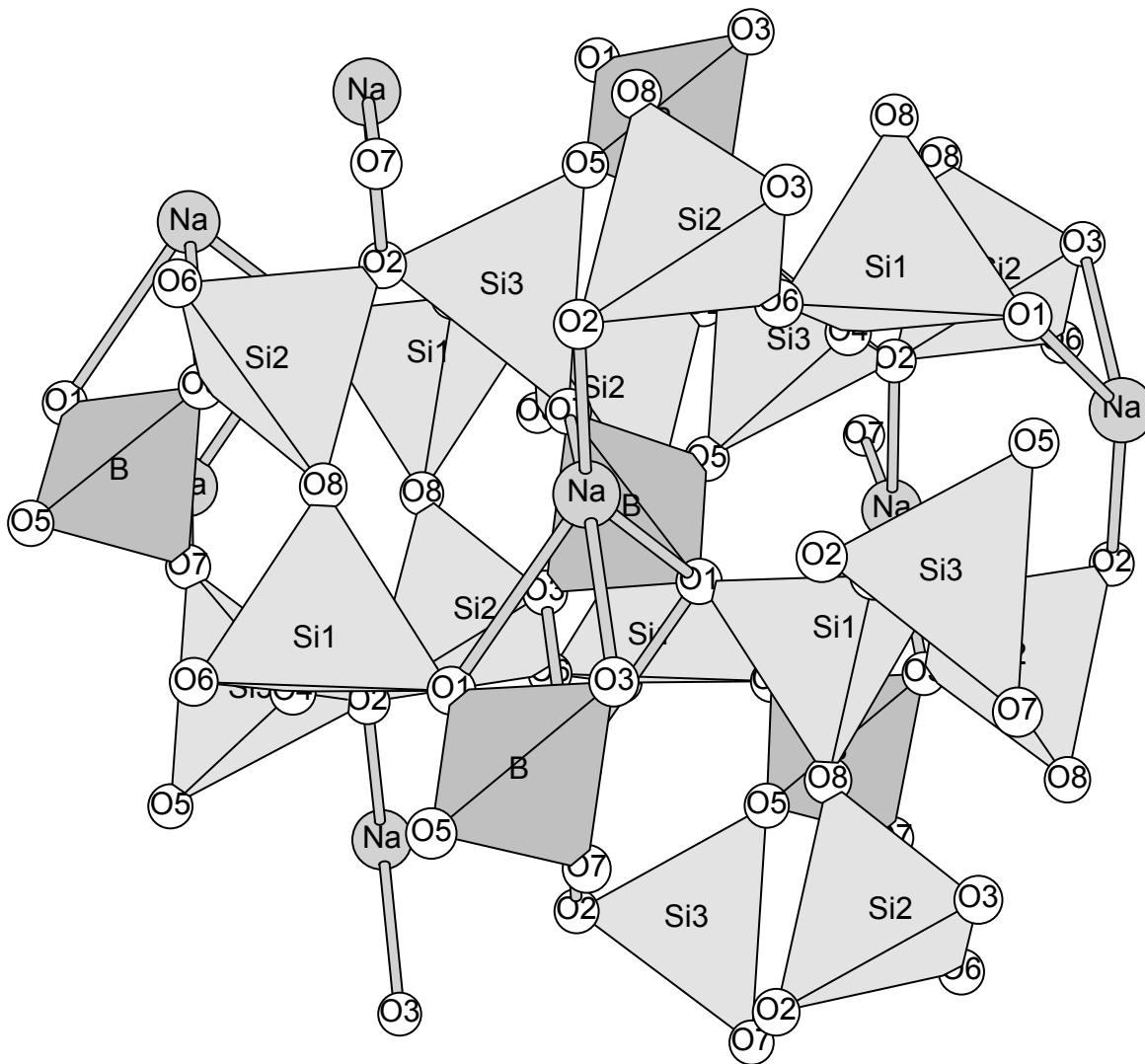


Fig. 1 Nanba et al.

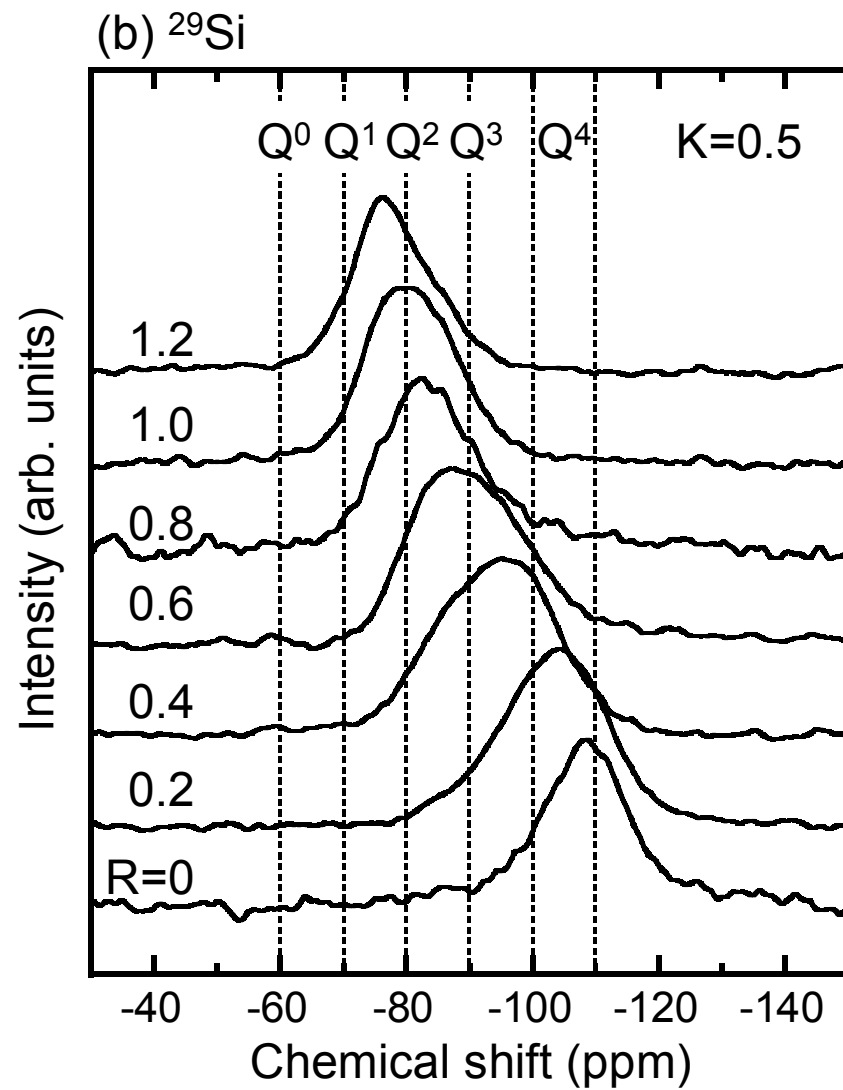
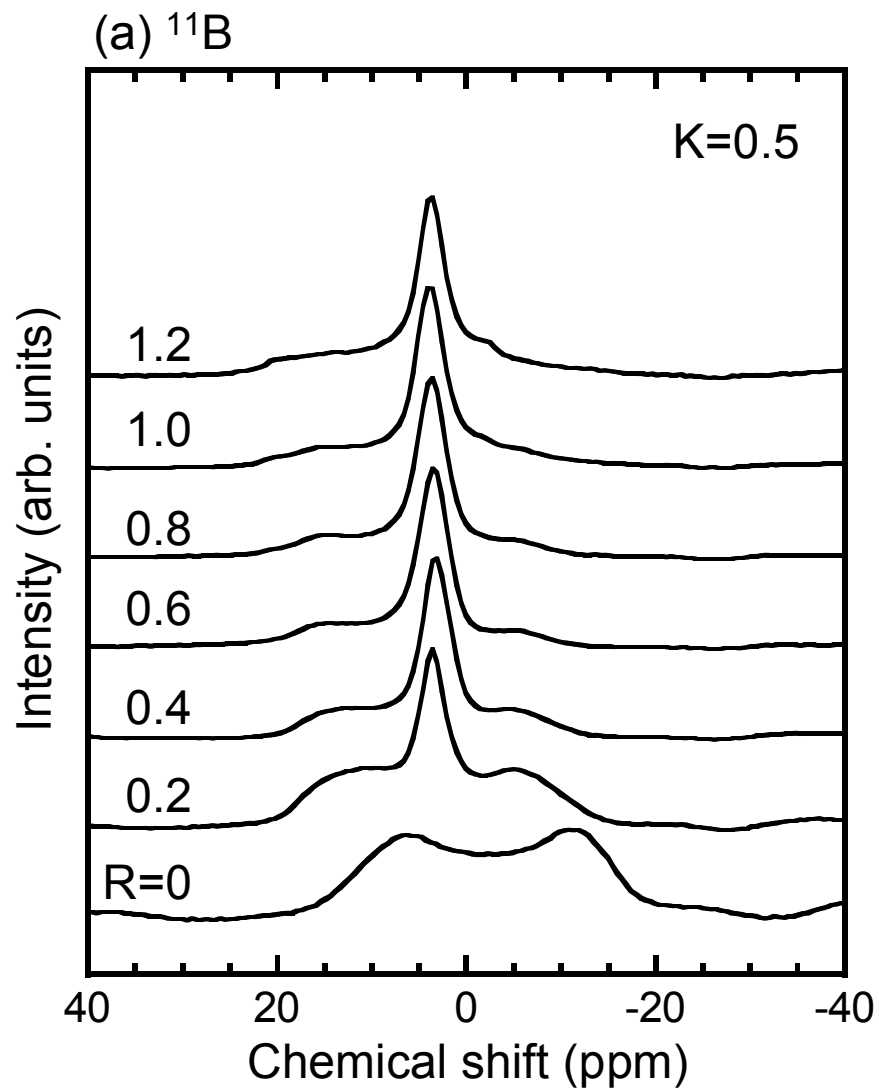


Fig. 2. Nanba et al

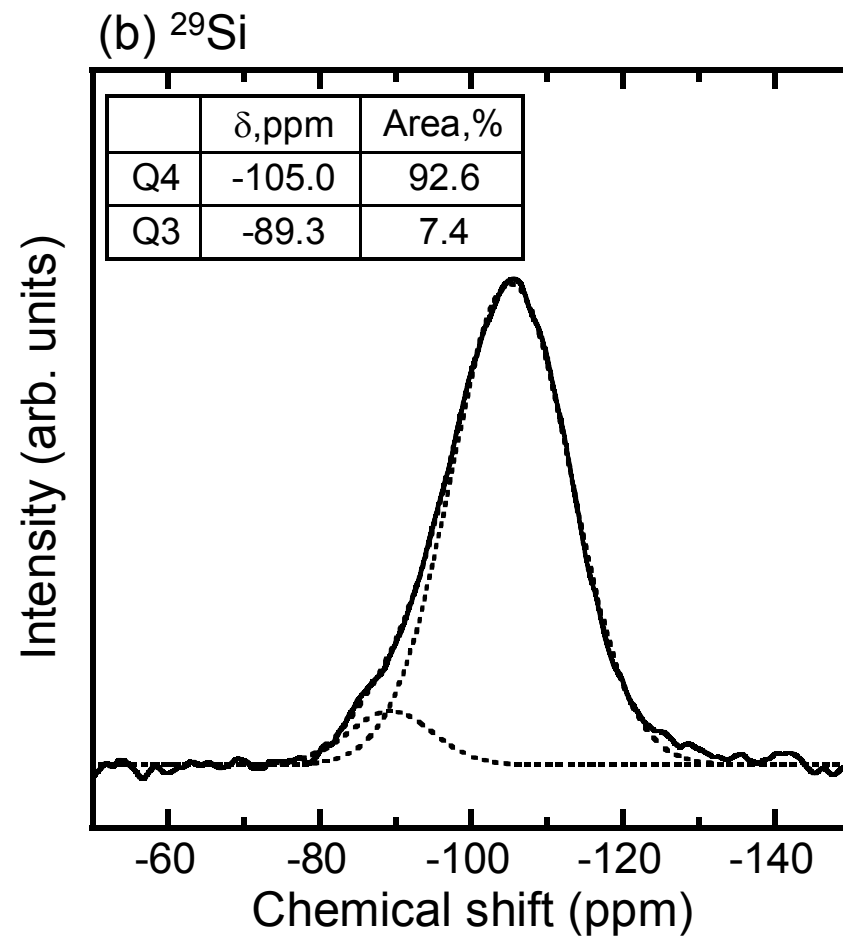
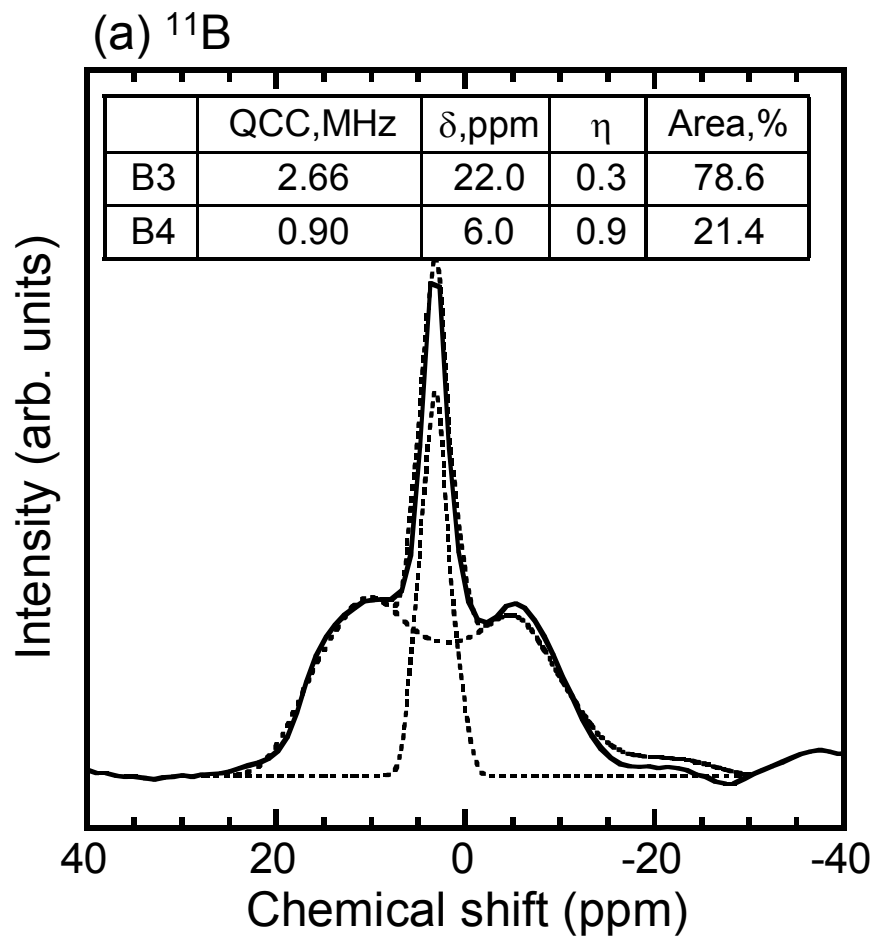


Fig. 3. Nanba et al

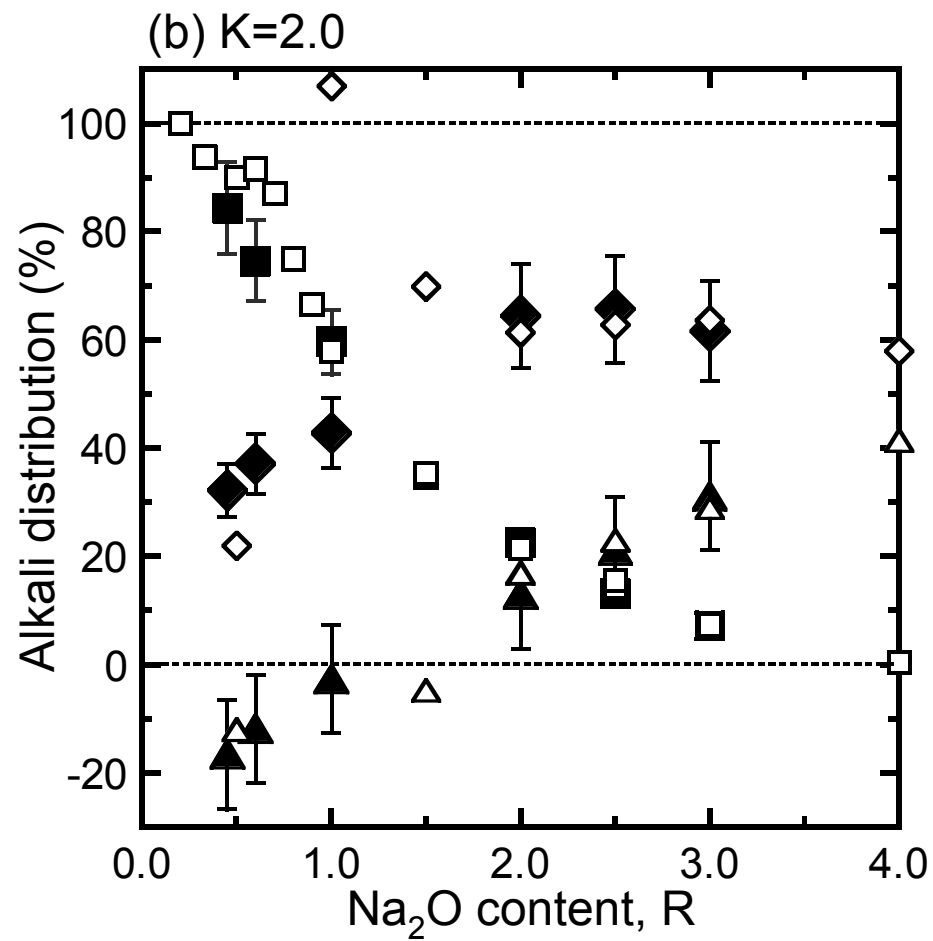
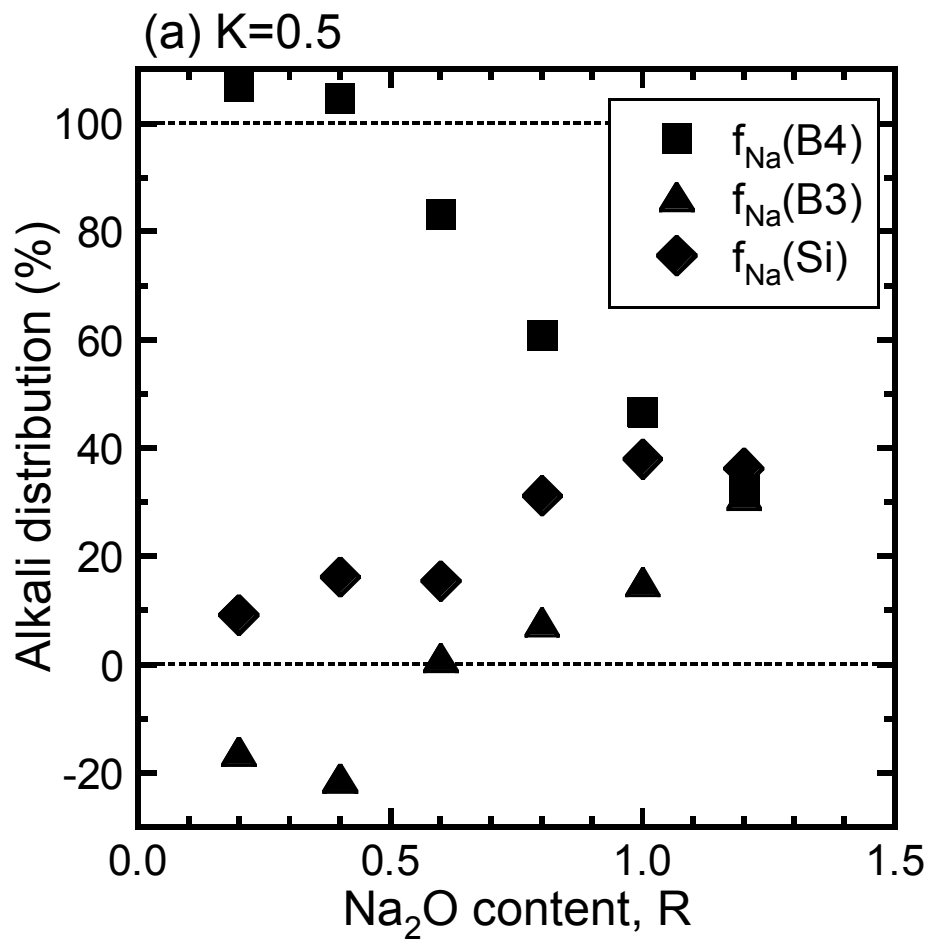


Fig. 4. Nanba et al

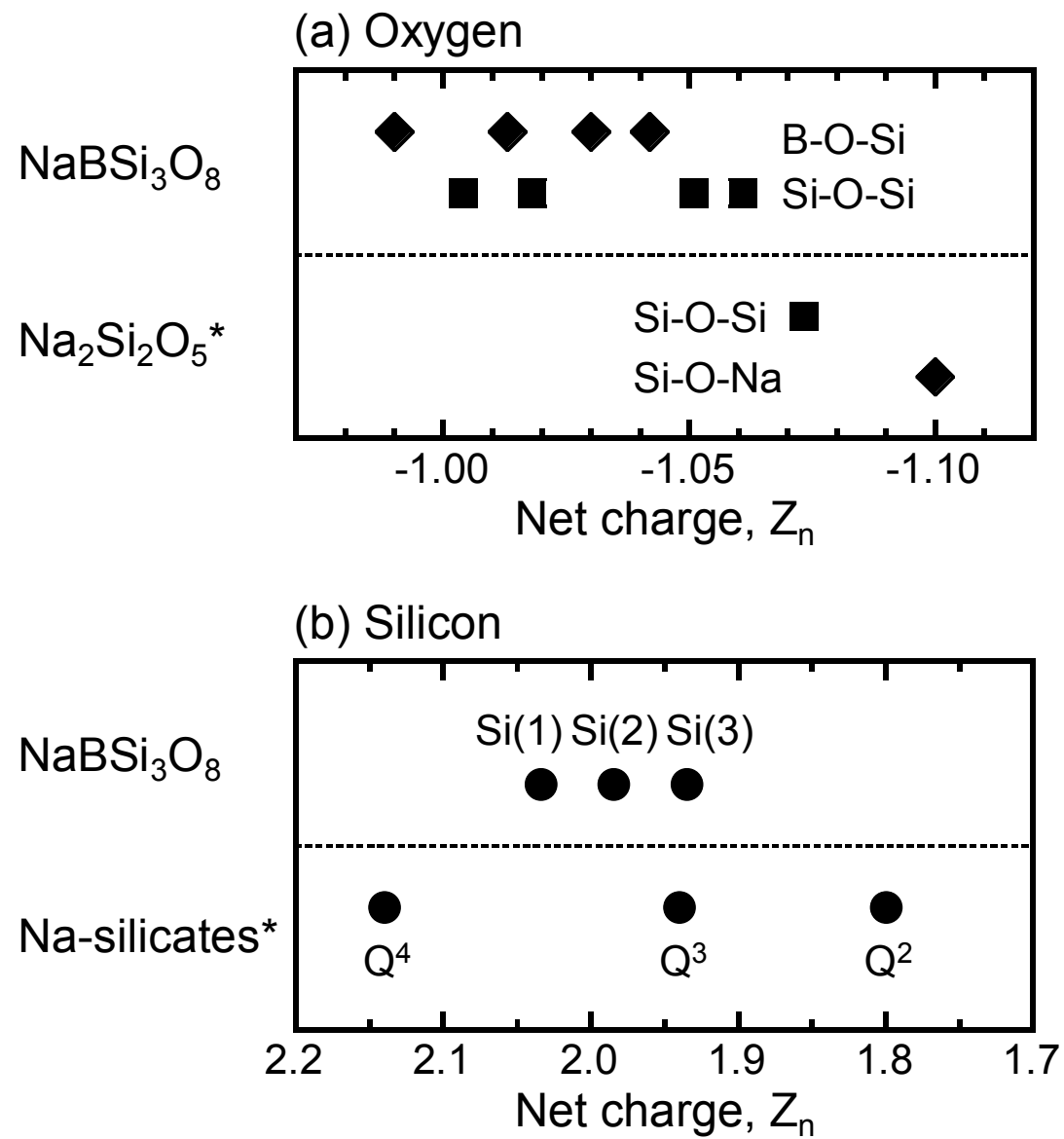


Fig. 5. Nanba et al

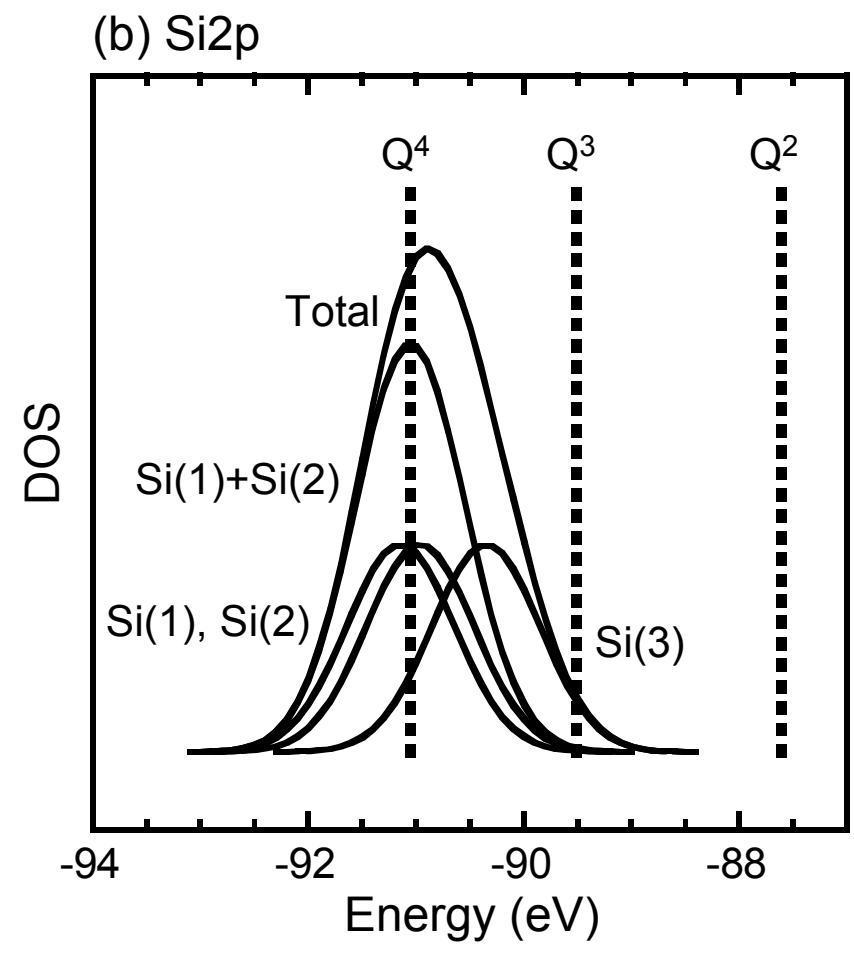
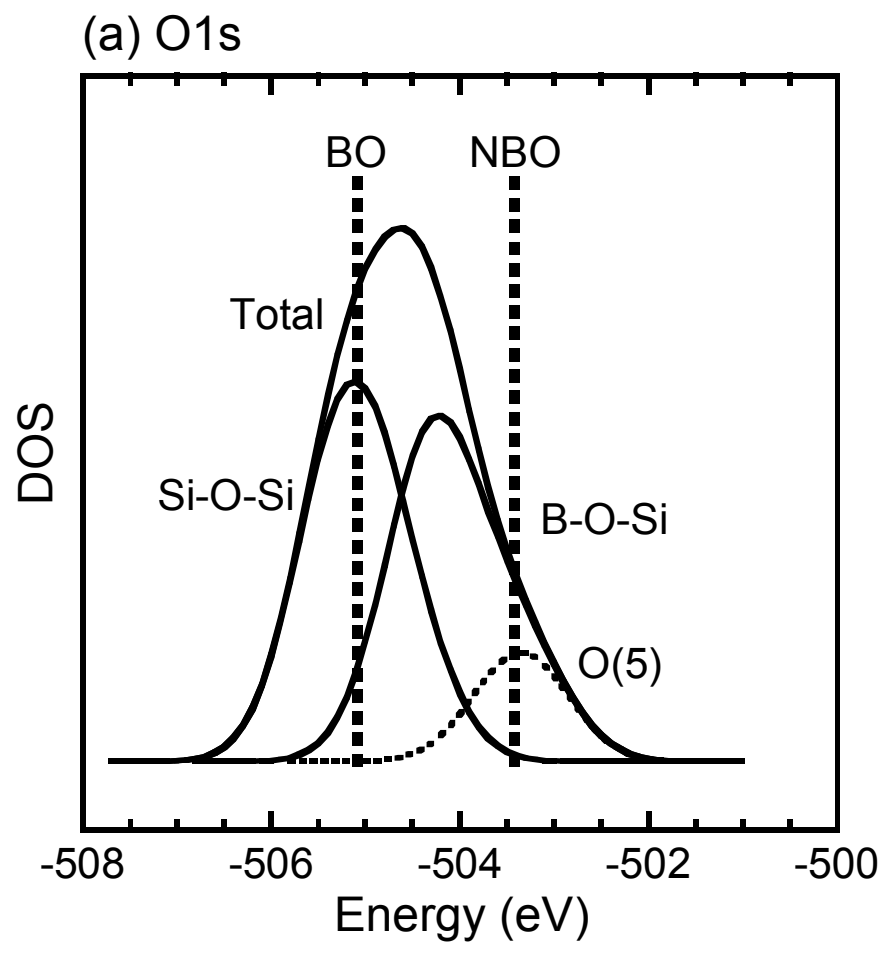


Fig. 6. Nanba et al

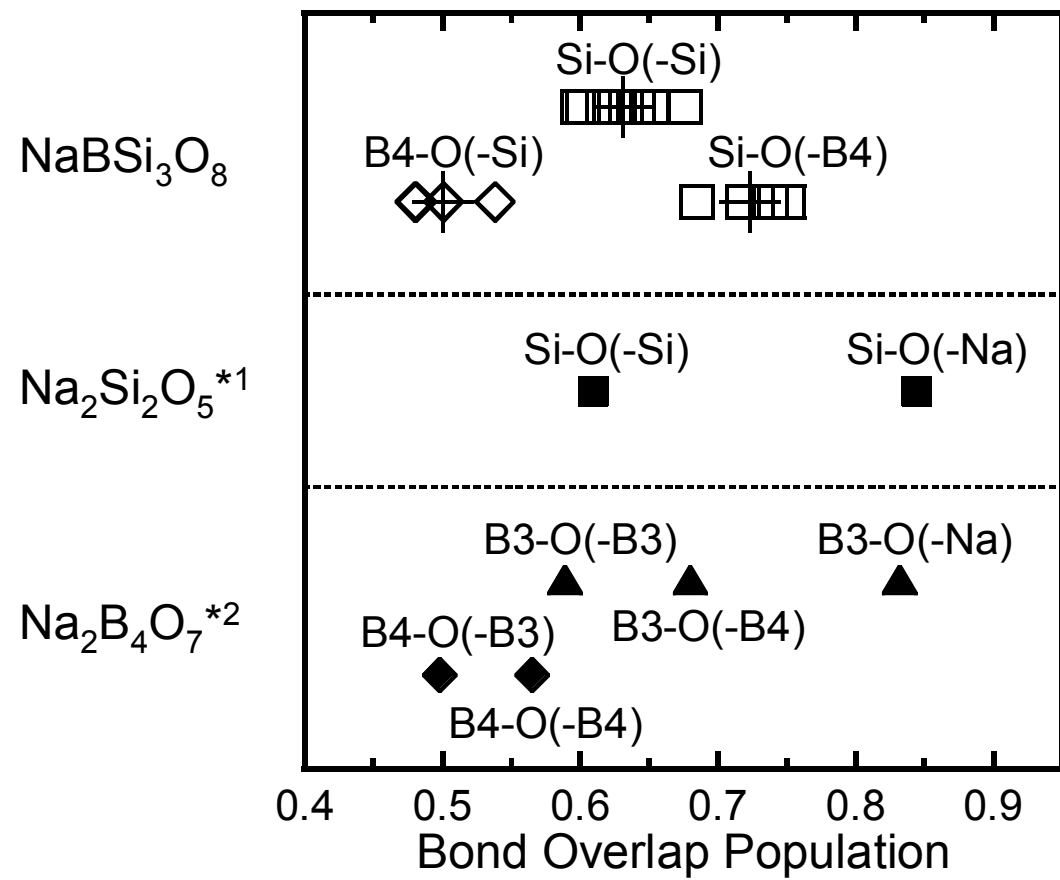


Fig. 7. Nanba et al